FULL PAPER

Dalton
www.rsc.org/dalton

A linear trinuclear mixed valence vanadium(V/IV/V) complex: synthesis, characterization, and solution behavior†

Yinshi Jin,[a] Hong-In Lee,[b] Myoungho Pyo[c] and Myoung Soo Lah*[a,d]

[a] *Department of Chemistry and Applied Chemistry, College of Science and Technology, Hanyang University, 1271 Sa-1-dong, Ansan, Kyunggi-do, 426-791, Korea. E-mail: mslah@hanyang.ac.kr; Fax: 82 31 407 3863; Tel: 82 31 400 5496*

[b] *Department of Chemistry Education, Kyungpook National University, Daegu, 702-701, Korea*

[c] *Department of Chemistry, Sunchon National University, Sunchon, 540-742, Korea*

[d] *Center for Bioactive Molecular Hybrids, Yonsei University, Seoul, 120-749, Korea*

Received 5th January 2005, Accepted 7th January 2005
First published as an Advance Article on the web 24th January 2005

The reaction between vanadium(III) acetylacetonate and *N*-hexanoylsalicylhydrazide (H_3hshz) yields a linear trinuclear mixed valence vanadium(V/IV/V) complex, V_3O_3(hshz)$_2$(OEt)$_2$, **1** (where hshz^{3-} is a triply deprotonated trianionic *N*-hexanoyl salicylichydrazidate), with a pseudo C_2 symmetry. A V(IV)O^{2+} group is at the center of complex **1** and is spanned by two terminal vanadium(V) ions with a square pyramidal geometry bridged *via* hydrazido ligands. In the crystalline form, the oxo group of the central vanadium(IV) ion is weakly coordinated to one of the terminal square pyramidal vanadium(V) ions of the neighboring trinuclear complex to form a dimeric structure. These dimers are linked *via* bis μ-alkoxo bridges to form a one-dimensional zigzag chain structure. In chloroform or methylene dichloride, the weak linkages between the trinuclear complexes present in the crystalline form are broken, and only the mixed valence trinuclear complex can be identified. In dimethyl sulfoxide or dimethylformamide, the trinuclear complex partially dissociates, and the unligated ligands remain in equilibrium with the trinuclear complex.

Introduction

There has been renewed interest in the chemistry of vanadium since the recognition of the involvement of vanadium ions in many important biological systems.[1] Vanadium has several oxidation states (−III to +V), of which, only vanadium(III), (IV), or (V) are found in biological systems.[2] Of these oxidation states, vanadium(IV) and (V) are the most common.[3] The distinctive preference of vanadium(IV) and (V) for N/O donor atoms has prompted the synthesis and characterization of many model complexes containing N/O donor ligands, and their spectroscopic properties and solution behavior have been investigated.[4] A study of mixed valence vanadium complexes shows that they possess distinctive bonding, chemistry, and applications.[5] However, the mixed valence chemistry of vanadium has developed slowly compared to developments in other early transition metals. Among the various types of mixed valence vanadium complexes reported so far, dinuclear mixed valence oxo-vanadium complexes containing a $[V_2O_3]^{3+}$ core represent the largest class because of their thermodynamic stability and ease of formation.[6] However, only a few trinuclear mixed valence vanadium complexes have been reported to date.[7] An understanding of the properties and behavior of high nuclearity vanadium complexes in both the solid state and in solution will provide great stimulus to research in the areas of biological and chemical catalysis.

In addition, it has been established that vanadium compounds possess insulin-mimetic properties.[8] The advantage of using vanadium complexes as diabetic drugs, is that they can be administered orally, thereby potentially eliminating (or reducing) the need for daily insulin injections for diabetic patients. Vanadium complexes possessing organic ligands are often less toxic than other types of vanadium complexes, and they can have an improved aqueous solubility and lipophilicity. The solution behavior of vanadium complexes is of special interest for their potential use as orally administrable diabetic drugs.

In this work, we report on the synthesis and structural characterization of a linear trinuclear mixed valence vanadium(V/IV/V) complex with multidentate N/O donor ligands, and on its solution behavior.

Experimental

Materials

The following reagents were used as received, with no further purification: salicylhydrazide (shz), hexanoyl chloride, vanadium(III) acetylacetonate, tetrabutylammonium tetrafluoroborate (TBABF$_4$), chloroform-*d*, methylene chloride-*d*, dimethyl sulfoxide (DMSO-*d*), and dimethylformamide (DMF-*d*), supplied by Aldrich Chemicals, and ethanol (EtOH), chloroform, methylene chloride, DMSO, and DMF supplied by Carlo Erba. The pentadentate ligand used, *N*-hexanoylsalicylhydrazide (H_3hshz), was synthesized by coupling salicylhydrazide and hexanoyl chloride.[9]

Instrumentation

The determination of the C, H, and N contents was performed at the Elemental Analysis Laboratory of the Korean Institute of Basic Science, Seoul. Infrared spectra were recorded using KBr pellets in the spectral range 4,000–600 cm^{-1} using a Bio-Rad FT-IR spectrophotometer. The absorption spectra of the samples were obtained using a Shimadzu UV-2401PC spectrophotometer. The ^{1}H NMR spectra of the samples were obtained using a Varian-300 spectrometer. The room temperature magnetic susceptibility of well-ground solid sample was measured using the Evans method.[10] All the electrochemical measurements were carried out at room temperature using a BAS CV-50W cell with a conventional three-electrode configuration. The working electrode used was a glassy carbon disk that was freshly polished with activated aluminum oxide before use. The reference and counter electrodes used were Ag/AgCl (3 M KCl) and Pt plates, respectively. All the potentials reported are referenced

† Electronic supplementary information (ESI) available: ^{1}H NMR and UV-Vis spectra for complex **1**. See http://www.rsc.org/suppdata/dt/b5/b500169m/

DOI: 10.1039/b500169m

to Ag/AgCl. To carry out the anaerobic voltammetric measurements, Ar gas was purged through the electrolyte media for at least 10 min until no O_2 redox pair was observed in the cyclic voltammograms. Anaerobic conditions were maintained throughout the measurements by providing a blanket of Ar gas. X-Band (9 GHz) EPR spectra were recorded on a Jeol (Japan) JES-TE300 ESR spectrometer using a 100-kHz field modulation. Low temperature spectra were obtained using a Jeol (Japan) ES-DVT3 variable temperature controller.

Synthesis

$V_3O_3(hshz)_2(OEt)_2$, **1**, (where $hshz^{3-}$ is a triply deprotonated trianionic *N*-hexanoyl salicylichydrazidate). A mass of 0.254 g (1.01 mmol) of H_3hshz (M = 250.30) was dissolved in 5 mL of ethanol. When 0.349 g (1.00 mmol) of vanadium(III) acetylacetonate was added to this solution, the color of the solution changed to a dark brown. The solution was filtered after stirring for 5 min, and slow evaporation of the filtrate yielded dark brown crystals after standing for 4 d (0.135 g, 52%). Anal. Calc. for $V_3O_3(hshz)_2(OEt)_2$ ($C_{30}H_{40}N_4O_{11}V_3$) (M = 785.48): C, 45.87; H, 5.13; N, 7.13. Found: C, 46.32; H, 5.40; N, 6.70%. IR (KBr, cm^{-1}): ν = 997, 981 and 960 for the three V=O groups. ^{1}H NMR (300 MHz, $CDCl_3$): δ 8.8–6.0 (br, 4H for phenyl protons); 5.6 (br, 2H, H at –COC(9)H_2–), 3.5 (br, 1H at $HOCH_2CH_3$ and/or 1H at V–OH); 3.72 (q, 2H for $HOCH_2CH_3$); 1.25 (t, 3H for $HOCH_2CH_3$), 1.44 (br, 6H, Hs at –$COCH_2$C(10)H_2C(11)H_2C(12)H_2–), 0.86 (br, 3H, H at –C(13)H_3). ^{1}H NMR (300 MHz, CD_2Cl_2): δ 8.6–6.2 (br, 4H for phenyl protons); 5.8 (br, 2H, H at –COC(9)H_2–), 3.65 (br, 2H for $HOCH_2CH_3$); 1.20 (br, 3H for $HOCH_2CH_3$), 1.7 (br, 6H, Hs at –$COCH_2$C(10)H_2C(11)H_2C(12)H_2–), 0.98 (br, 3H, H at –C(13)H_3). ^{1}H NMR (300 MHz, d_6-DMSO): observed as a mixture of ligand, complex **1**, and unligated ethanol in a 1 : 3 : 1 ratio. Bands for ligand: δ 11.93, 10.52, 10.12 (s, s, s, 3H, Hs at amides and phenolic OH), 7.88 (d, 1H, H at phenyl), 7.44 (t, 1H, H at phenyl), 6.97–6.90 (m, 2H, Hs at phenyl), 2.20 (t, 2H, H at –COC(9)H_2–), 1.56 (m, 2H, H at $COCH_2$C(10)H_2), 1.29 (m, 4H, H at $COCH_2CH_2$C(11)H_2C(12)H_2), 0.88 (t, 3H, J = 6.8 Hz, H at C(13)H_3). Bands for unligated ethanol: 3.73 (br), 1H at $HOCH_2CH_3$ and 2H at H_2O; 3.44 (q), 2H at $HOCH_2CH_3$; 1.05 (t), 3H at $HOCH_2CH_3$. Bands for complex **1**: δ 8.05–7.85 (m, 1H, H at phenyl), 7.65–7.30 (m, 1H, H at phenyl), 7.15–6.65 (m, 2H, Hs at phenyl), 5.6 (m, 2H at COC(9)H_2), 2.75–2.55 (m, 2H, H at $COCH_2$C(10)H_2), 1.47 (m, 2H, H at $COCH_2CH_2$C(11)H_2), 1.29 (m, 2H, H at $COCH_2CH_2CH_2$C(12)H_2), 0.88 (t, 3H, H at –C(13)H_3). ^{1}H NMR (300 MHz, d_7-DMF): observed as a mixture of ligand, complex **1**, and unligated ethanol in a 1 : 2 : 1 ratio. Bands for ligand: δ 12.25, 10.68, 10.16 (s, s, s, 3H, Hs at amides and phenolic OH), 8.0–6.2 (br, 4H for phenyl protons), 2.33 (t, 2H, H at –COC(9)H_2), 1.57 (m, 2H, H at –$COCH_2$C(10)H_2–), 1.36 (m, 4H, H at –$COCH_2CH_2$C(11)H_2C(12)H_2–), 0.91 (t, 3H, J = 6.8 Hz, H at –C(13)H_3). Bands for complex **1**: δ 8.0–6.2 (br, 4H for phenyl protons), 6.0–5.6 (br, 2H at –COC(9)H_2– and 2H at H_2O), 4.2–4.6 (br, 2H, H at $COCH_2$C(10)H_2), 1.57 (br, 2H, H at –$COCH_2CH_2$C(11)H_2–), 1.36 (br, 2H, H at –$COCH_2CH_2CH_2$C(12)H_2–), 0.91 (br, 3H, H at –C(13)H_3). Bands for unligated ethanol: δ 3.56 (q), 2H at $HOCH_2CH_3$; 1.13 (t), 3H at $HOCH_2CH_3$. UV-Vis ($CHCl_3$) [λ_{max} (ε)]: 300 nm (23,000 M^{-1} cm^{-1}), 330 nm (shoulder, 15,000 M^{-1} cm^{-1}). UV-Vis (CH_2Cl_2) [λ_{max} (ε)]: 300 nm (28,000 M^{-1} cm^{-1}), 330 nm (shoulder, 21,000 M^{-1} cm^{-1}). UV-Vis (DMSO) [λ_{max} (ε)]: 290 nm (19,000 M^{-1} cm^{-1}), 305 nm (shoulder, 17,000 M^{-1} cm^{-1}), 340 nm (shoulder, 8,000 M^{-1} cm^{-1}). UV-Vis (DMF) [λ_{max} (ε)]: 290 nm (22,000 M^{-1} cm^{-1}), 305 nm (shoulder, 19,000 M^{-1} cm^{-1}), 340 nm (shoulder, 9,000 M^{-1} cm^{-1}).

X-Ray crystallography

A dark brown crystal of complex **1** was mounted on a glass fiber. Preliminary examination and data collection were performed using a Bruker SMART CCD Detector single crystal X-ray diffractometer employing a graphite monochromated Mo-Kα radiation source (λ = 0.71073 Å) equipped with a sealed tube X-ray source operating at −100 °C for **1**. Preliminary unit cell constants were determined using a set of 45 narrow frame scans (0.3° in ω). The data sets collected consisted of 1,286 frames of intensity data, collected using a frame width of 0.3° in ω, and a count time of 10 s $frame^{-1}$ with a crystal to detector distance of 5 cm. The double pass scanning method was used to exclude any noise. The collected frames were integrated using an orientation matrix determined from the narrow frame scans. The SMART and SAINT software packages[11] were used for data collection and integration, respectively. Analysis of the integrated data did not show any decay. The final cell constants were determined using a global refinement of 8,192 reflections (θ < 25.0°). Collected data were corrected for absorbance using the SADABS package[12] based upon the Laue symmetry using equivalent reflections. The structural solution and refinement of the structure were carried out using the SHELXTL v5.1 software package.[13] All the non-hydrogen atoms were refined anisotropically. The hydrogen atoms were assigned isotropic displacement coefficients, U(H) = 1.2U(C) or 1.5 U(C_{methyl}), and their coordinates were allowed to move on their respective atoms using the SHELXTL v5.1 software routines. The crystal and intensity data obtained are shown in Table 1.

CCDC reference number 249323.

See http://www.rsc.org/suppdata/dt/b5/b500169m/ for crystallographic data in CIF or other electronic format.

Table 1 Crystal data and structure refinement for complex **1**

Empirical formula	$C_{30}H_{40}N_4O_{11}V_3$
M	785.48
T/K	173(2)
Crystal system	Triclinic
Space group	$P\bar{1}$
a/Å	9.407(2)
b/Å	14.364(4)
c/Å	14.709(4)
α/°	65.655(4)
β/°	89.823(4)
γ/°	75.980(4)
V/Å^3	1746.2(8)
Independent reflections	8352 [R(int) = 0.1038]
Absorption correction	Semi-empirical from equivalents
Goodness-of-fit on F^2	1.031
Final R indices [$I > 2\sigma(I)$][a,b]	$R1$ = 0.0812, $wR2$ = 0.1777
R indices (all data)	$R1$ = 0.1797, $wR2$ = 0.2243
Largest diff. peak and hole/e Å^{-3}	0.716 and −0.922

[a] $R1 = \Sigma \|F_o| - |F_c\| / \Sigma |F_o|$. $wR2 = [\Sigma w(F_o^2 - F_c^2)^2 / \Sigma w F_o^4]^{1/2}$. [b] The crystallographic R factors were higher than usually obtained for well-defined structures. The crystal obtained was in the form of a thin plate (0.30 × 0.12 × 0.03 mm), which did not diffract well (only 3,812 reflections among the 8,352 unique reflections up to 2θ = 56° were observed). However, no significant residual electron densities were observed, except for a few electron densities close to the vanadium ions. The largest electron density of 0.716 e Å^{-3} was in the vicinity of the vanadium ion. The standard deviation of the bond distances and angles was in the range 0.005–0.008 Å in bond distance, and 0.08–0.09° in bond angle. These values indicate that the crystal structure was reasonably well defined. When the refinement was performed with the reflections up to 2θ = 46°, the value of $R1$ = 0.0679 for 3,221 reflections with $F_o > 4\sigma(F_o)$ was much lower than that of $R1$ = 0.0812 for 3,812 reflections with $F_o > 4\sigma(F_o)$ for 2θ = 56°. However, the standard deviation of the bond distances and angles in the 2θ = 46° data was higher than that in the 2θ = 56° data.

Results and discussion

Preparation and characterization of complex 1

The mixed valence vanadium complex, $V_3O_3(hshz)_2(OEt)_2$, was synthesized using vanadium(III) acetylacetonate and *N*-hexanoylsalicylhydrazide (H_3hshz) in ethanol (Scheme 1). The

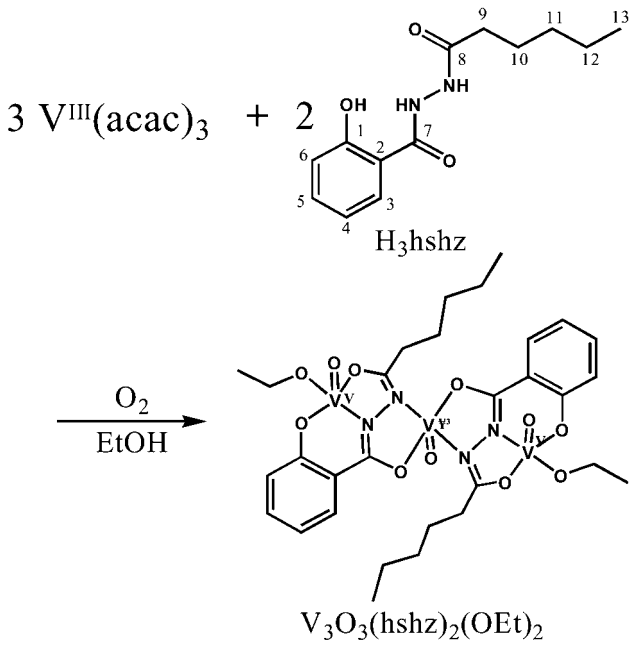

Scheme 1

IR spectrum of complex **1** in a KBr pellet exhibited three characteristic V=O stretch bands at 997, 981, and 960 cm^{-1}, which suggest that there are three different V=O groups in the solid state[14] (Fig. 1). The magnetic susceptibility of complex **1** (μ_{eff} = 1.79 μ_B after applying a diamagnetic correction using Pascal's constants) suggests that the trinuclear complex contains one paramagnetic d^1 vanadium(IV) ion. During the reaction, the vanadium ion was air-oxidized from its initial +III oxidation state to the final mixed valence vanadium(V/IV/V) oxidation states observed in ethanol solution.

Crystal structure of complex 1

An ORTEP drawing of complex **1** is shown in Fig. 2. Complex **1** is a linear trinuclear mixed valence vanadium(V/IV/V) complex,

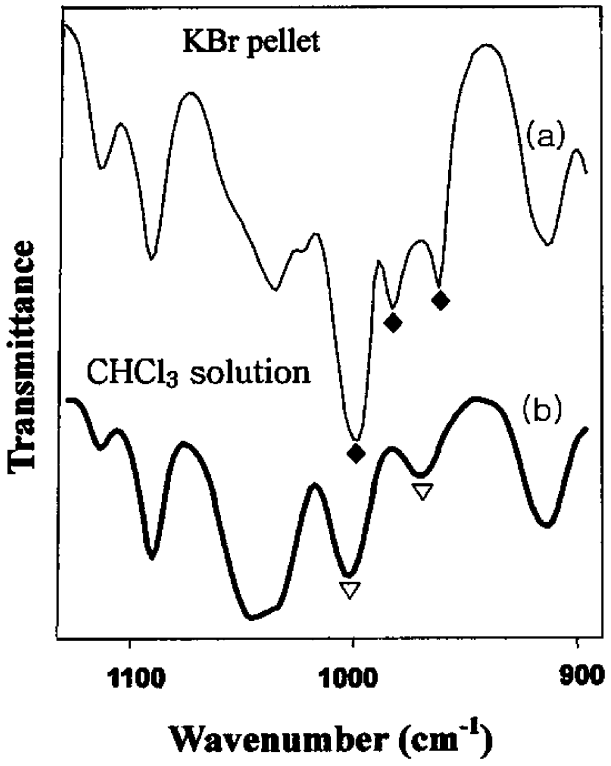

Fig. 1 (a) IR spectra of complex **1**, $V_3O_3(hshz)_2(OEt)_2$ in a KBr pellet, and (b) in a chloroform solution.

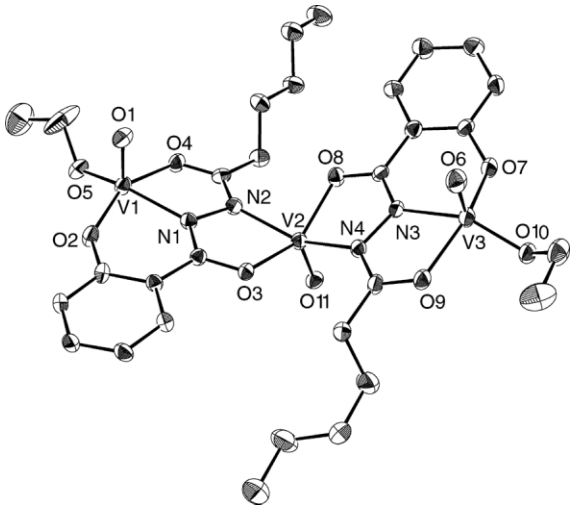

Fig. 2 ORTEP drawing of complex **1**.

with pseudo C_2 symmetry. In complex **1**, a vanadium(IV) ion is at the molecular center, and is spanned by two terminal vanadium(V) ions with a square pyramidal geometry bridged *via* hydrazido ligands.

The geometry of the terminal vanadium metal centers is of monooxo-, alkoxo-bound square pyramids. Triply deprotonated trianionic *N*-hexanoylsalicylhydrazidate ($hshz^{3-}$) is coordinated to the terminal vanadium ions as a tridentate ligand to form five- and six-membered chelating rings using an iminophenolate group (O2 and N1 atoms) and an iminohexanoxylate group (N1 and O4 atoms) of the ligand in the meridional mode. The remaining basal site of the square pyramid of the terminal vanadium ions is occupied by an ethoxide anion. The vanadium–ethoxy oxygen bond lengths (V1–O5, 1.750(5) Å; V3–O10, 1.765(4) Å) are about 0.2 Å shorter than the vanadium–oxylate group oxygen atom bond lengths (V1–O4, 1.972(5); V3–O9, 1.967(5) Å) (Table 2). The vanadium–oxo bond length (V1–O1, 1.577(5) Å; V3–O6, 1.561(5) Å) is similar to reported values for analogous structures.[15] Each terminal vanadium ion is displaced by 0.358(3) Å (O1 atom) and 0.374(3) Å (O6 atom) from the corresponding basal plane of the square pyramid. The oxidation states of the terminal vanadium ions were assigned as +V, based on the crystal data and the value of the magnetic moment of the trinuclear complex. It is well known that the oxo and alkoxo groups can stabilize the high oxidation states of vanadium complexes.[4f,16]

The square planar coordination sites of the central square pyramidal vanadium ion are occupied by the two hydrazidate groups (O3, N2 and N4, O8 atoms) of the terminal $hshz^{3-}$ ligands in a *trans* fashion to form two five-membered chelating rings; an oxo group occupies the remaining axial site of the square pyramid. The central vanadium metal ion is also displaced by 0.606(3) Å from the basal plane of the square pyramid. The configuration of the central vanadium ion was assigned as being d^1, corresponding to the +IV oxidation state.

In the crystalline form, the oxo group of the central vanadium(IV) ion is weakly coordinated to one of the terminal square pyramidal vanadium(V) ions of the neighboring trinuclear complex (V1a–O11, 2.525(4) Å) to form two μ-oxo bridged (V2–O11–V1a, 166.4(3)°; V1a · · · V2, 4.082(2) Å) hexanuclear cluster. This is a dimer of the trinuclear complex (Fig. 3). These dimers are linked *via* bis μ-alkoxo bridges (V3–O10, 1.765(4) Å; V3b–O10, 2.576(5) Å; V3–O10–V3b, 107.6(2)°; V3 · · · V3b, 3.537(2) Å) to form a zigzag-type one-dimensional chain. While the geometry of the central vanadium(IV) ion is square pyramidal, the geometry of the terminal vanadium(V) ions is that of a distorted octahedron. However, the distorted octahedral local environments of the two terminal vanadium(V) ions are slightly different in the crystalline structure.

Table 2 Selected bond lengths [Å] and angles [°] for complex **1**

V(1)–O(1)	1.577(5)	V(3)–O(6)	1.561(5)	V(2)–O(11)	1.585(4)	V(1)–N(1)	2.049(5)
V(1)–O(5)	1.750(5)	V(3)–O(10)	1.765(4)	V(2)–O(3)	1.950(4)	V(3)–N(3)	2.057(5)
V(1)–O(2)	1.818(5)	V(3)–O(7)	1.837(5)	V(2)–O(8)	1.957(5)	V(2)–N(2)	2.051(5)
V(1)–O(4)	1.972(5)	V(3)–O(9)	1.967(5)	V(1)–V(2)	4.082(2)	V(2)–N(4)	2.045(5)
V(1)–O(11)	2.525(4)	V(3)–O(10)	2.576(5)	V(3)–V(3)	3.536(2)		
O(1)–V(1)–O(5)	102.4(2)	O(6)–V(3)–O(10)	105.6(2)	O(11)–V(2)–O(3)	110.1(2)	N(4)–V(2)–N(2)	149.9(2)
O(1)–V(1)–O(2)	103.8(2)	O(6)–V(3)–O(7)	101.0(3)	O(11)–V(2)–O(8)	110.8(2)	O(9)–V(3)–N(3)	74.3(2)
O(5)–V(1)–O(2)	103.1(2)	O(10)–V(3)–O(7)	102.0(2)	O(3)–V(2)–O(8)	139.09(19)	O(4)–V(1)–N(1)	74.2(2)
O(1)–V(1)–O(4)	97.5(2)	O(6)–V(3)–O(9)	97.2(3)	O(11)–V(2)–N(4)	102.8(2)	O(2)–V(1)–N(1)	83.9(2)
O(5)–V(1)–O(4)	90.3(2)	O(10)–V(3)–O(9)	91.5(2)	O(3)–V(2)–N(4)	94.23(19)	O(7)–V(3)–N(3)	83.3(2)
O(2)–V(1)–O(4)	151.7(2)	O(7)–V(3)–O(9)	153.4(2)	O(8)–V(2)–N(4)	77.53(19)	O(8)–V(2)–N(2)	90.0(2)
O(1)–V(1)–N(1)	99.2(2)	O(6)–V(3)–N(3)	100.9(2)	O(11)–V(2)–N(2)	107.3(2)	V(1)–O(11)–V(2)	166.4(3)
O(5)–V(1)–N(1)	154.8(2)	O(10)–V(3)–N(3)	151.3(2)	O(3)–V(2)–N(2)	77.33(19)	V(3)–O(10)–V(3)	107.6(2)

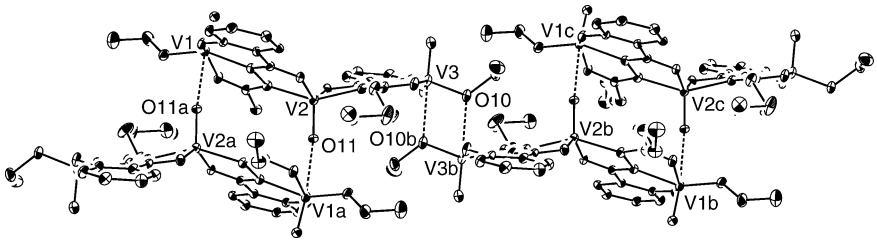

Fig. 3 The formation of a zigzag-type one-dimensional chain *via* the two different types of linkage: a cyclic linkage formation *via* two μ-oxo bridges between the oxo atom of the central vanadium(IV) ion and one terminal vanadium(V) ion, and the formation of a linear linkage *via* the bis μ-alkoxo bridges between the other terminal vanadium(V) ions.

Solution behavior of complex 1

The IR spectrum of complex **1** in chloroform shows two V=O stretch bands at 1,002 and 970 cm^{-1}, which suggests that two different V=O groups exist in solution (Fig. 1). The local dissimilarity of the two terminal vanadium centers from the μ-oxo or μ-alkoxo bridging interactions in the solid state disappears, which suggests that the complex exists as an isolated trinuclear form in chloroform.

The ^{1}H NMR spectrum of complex **1** in chloroform can be assigned to the paramagnetic trinuclear mixed valence vanadium complex‡ (Fig. 4a). The broad phenyl protons of the complex were observed at around 8.8–6.0 ppm. The methylene (C9) protons that are closest in distance from the vanadium(IV) center were observed at around 5.6 ppm. The remaining aliphatic protons were observed at around 1.25–0.86 ppm. The sharp peaks observed at 3.72 and 1.25 ppm were assigned to free, non-ligated ethanol that is most likely to be formed *in situ* in solution. However, the ^{1}H NMR spectrum of complex **1** in DMSO yielded two sets of bands in an approximate 1 : 3 ratio (Fig. 4b). The set of sharp signals denoted by the open triangles corresponds to the free H_3hshz ligand and ethanol. The broad signals denoted by the filled diamonds were assigned to the paramagnetic trinuclear mixed valence vanadium(V/IV/V) complex. Four broad multiplet signals at around 8.05–6.65 ppm were assigned for the four phenyl protons of the complex. The broad multiplet at 5.6 ppm was assigned to the methylene (C9) protons that form the closest bonding links to the vanadium(IV) center, as in chloroform. The two multiplets at 2.75–2.55 and 2.47 ppm were assigned to the bands from the next four ethylene (C10 and C11) protons. The two protons of the C12 methylene group and the three methyl protons appear at the same chemical shift positions (1.29 and 0.88 ppm) as those of the free ligand protons. Sharp peaks at 3.44 and 1.05 ppm from the protons of free, non-ligated ethanol were observed, as in chloroform.

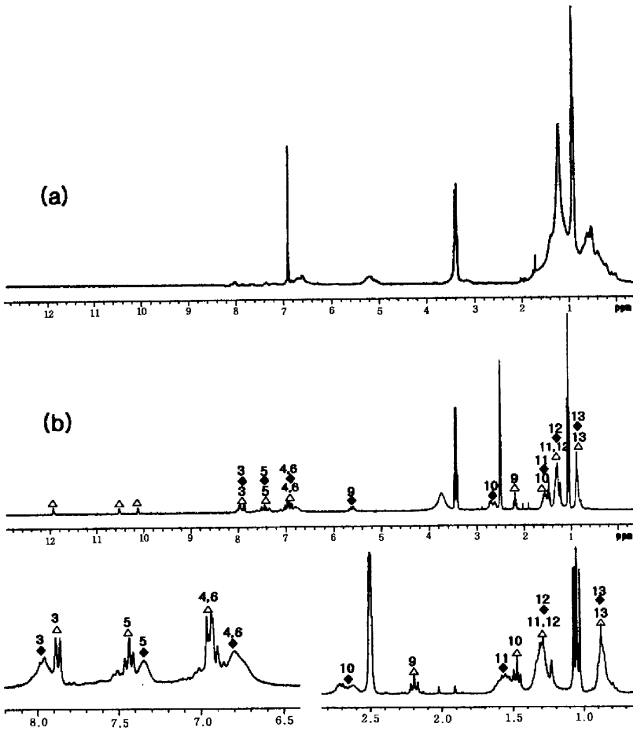

Fig. 4 (a) ^{1}H NMR spectrum of complex **1** in $CDCl_3$. (b) ^{1}H NMR spectrum of complex **1** in DMSO-*d*. The set of sharp bands denoted by the open triangles corresponds to the free H_3hshz ligand and ethanol. The broad bands denoted by the filled diamonds correspond to the paramagnetic trinuclear mixed valence vanadium(V/IV/V) complex. The mixing of the bands at 1.29 and 0.88 ppm shows that the bands from the two species overlap at some positions. The two lower spectra show an expanded view of the peaks from the four phenyl protons and the aliphatic protons.

‡ The detailed assignment of each proton signal of complex **1** in chloroform was difficult because of the broadening and overlap of the signals. However, the general feature of the spectrum resembles that of complex **1** in DMSO.

The ethoxide may accept a proton from the water present in the complex. The absence of signals corresponding to bound ethoxide, which usually appear at 5.39 and 1.57 ppm,[15b] supports

this supposition.§ Even though the peaks for the complex in chloroform are much broader than those in DMSO, the general features of the trinuclear complex in each solution are very similar. While there is no evidence for the presence of free dissociated ligands in chloroform solution, in DMSO the trinuclear vanadium complex partially dissociates and the liberated free ligands remain in equilibrium with the undissociated trinuclear complex. Similar solution behavior was observed in non-coordinating dichloromethane solvent and in the coordinating DMF solvent. In dichloromethane, the signals observed were similar to those from complex **1** in chloroform, suggesting the existence of an identical species. However, in DMF, two sets of bands corresponding to the vanadium complex and to the free ligand were observed, as was observed in DMSO (Fig. S1†).

While the UV-Vis spectrum of complex **1** in chloroform (Fig. S2†) shows two ligand to metal charge transfer bands at 300 nm (23,000 M^{-1} cm^{-1}) and 330 nm (shoulder, 15,000 M^{-1} cm^{-1}), the UV-Vis spectrum in DMSO shows similar charge transfer bands at approximately 305 nm (shoulder, 17,000 M^{-1} cm^{-1}) and 340 nm (shoulder, 8,000 M^{-1} cm^{-1}), but with rather smaller absorption coefficients. The partial dissociation of the trinuclear vanadium complex in DMSO results in a decrease in the absorption coefficients of the charge transfer bands. As was seen in the NMR data, the absorption coefficients in non-coordinating solvents, such as dichloromethane and chloroform, are similar, but the absorption coefficients in coordinating solvents, such as DMSO and DMF, are much reduced when compared to those of non-coordinating solvents. This observation agrees with the proposed ligand dissociation scheme based on the NMR experimental results, where the trinuclear vanadium complex partially dissociates in coordinating solvents and is in equilibrium with the free ligand.

Cyclic voltammetric measurements were performed in a chloroform solution containing complex **1** (5 mM, 10 mM, and 20 mM) and 0.1 M $TBABF_4$ (Bu_4NBF_4) using a scan rate of 10 mV s^{-1}. The concentration-dependent cyclic voltammograms suggest that the reduction peak occurring at a potential of *ca.* −480 mV and the oxidation peak occurring at a potential of *ca.* 550 mV arise from complex **1** (Fig. 5). The irreversible reduction potential occurring at a potential of −480 mV is assigned to the terminal dialkoxo monooxo square pyramidal V(V) center.[17] The effect of the dialkoxo monooxo groups on the reduction potential is comparable to that of the monoalkoxo dioxo groups.[18] It is likely that the irreversible oxidation peak occurring at a potential of 550 mV results from the V(IV)/V(V) redox couple of the central V(IV) ion.[19] These assignments agree with the ratio of the anodic and cathodic currents, which corresponds to the ratio of the vanadium(IV) and vanadium(V) centers (see the inset of Fig. 5). When 10% (v/v) ethanol was added to a solution of 20 mM of complex **1**, the oxidation peak occurring at a potential of 550 mV shifted to a lower potential at *ca.* 470 mV. This result indicates that the coordination number of the central vanadium(IV) ion increased to six by bonding with the ethanol in the $CHCl_3$/EtOH mixed solvent. A similar variation in the reduction potentials of the vanadium complex dependency on the coordination environment has been reported previously.[4a,14b,17a,18] The reduction peak occurring at a potential of −480 mV also shifted to a higher potential at *ca.* −310 mV,

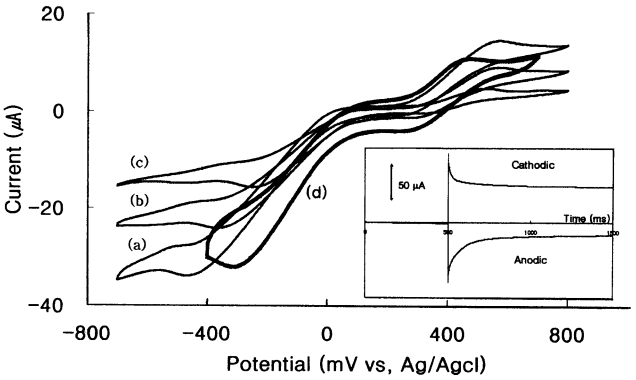

Fig. 5 Cyclic voltammograms of a complex **1**/0.1 M $TBABF_4$/chloroform solution scanned at 10 mV s^{-1}. (a) 20 mM of complex **1**, (b) 10 mM of complex **1**, (c) 5 mM of complex **1**, and (d) after addition of ethanol (10 vol% ethanol : chloroform solution) to the solution of 20 mM of complex **1**. The inset represents the anodic and cathodic current of complex **1**. The ratio of the cathodic current to the anodic current was *ca.* 2.8.

which indicated a change in the coordination environment of the terminal vanadium(V) ion.

Fig. 6 shows the $S = 1/2$ EPR spectra of complex **1** in both the solid and the frozen solution states, and these data are consistent with the observed magnetic moment value of

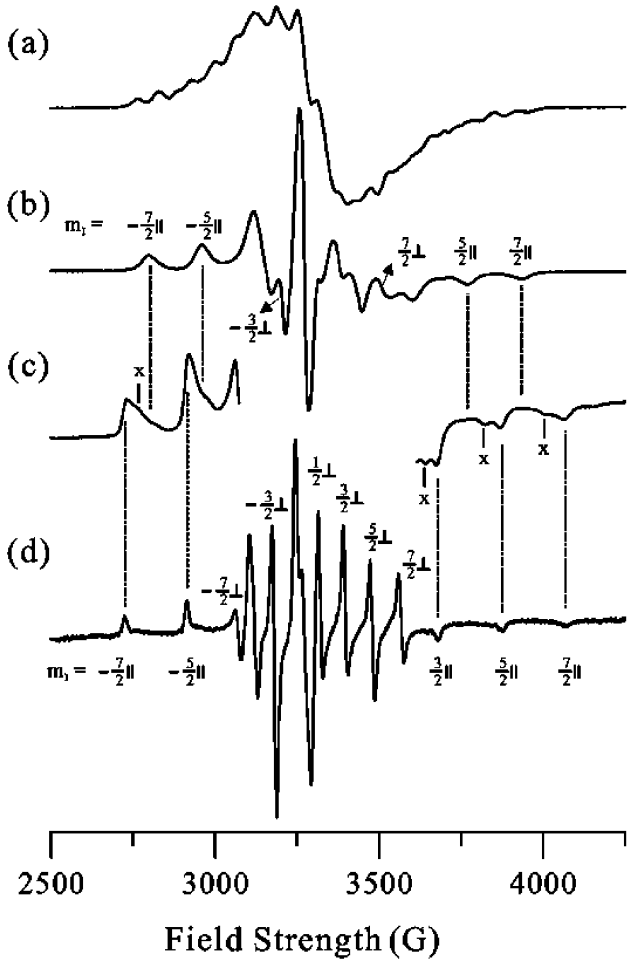

Fig. 6 EPR spectra of: (a) a powdered sample of complex **1** at room temperature, (b) 1.2 mM of complex **1** in chloroform at 120 K, (c) 2.5 mM of complex **1** in DMSO at 120 K, and (d) 0.25 (= 2.5/10) mM of complex **1** in DMSO at 120 K. The central region has been omitted for clarity in 6(c). The apparent $A_\parallel$ and $A_\perp$ lines are labeled according to the m_I values in (b) and (d). The experimental parameters used are: microwave frequency = (a) 9.215 and (b)–(d) 9.216 GHz; microwave power = (a) 0.1 and (b)–(d) 1 mW; modulation width = (a) 4 and (b)–(d) 2 G; time constant = 0.3 s; scan time = (a) 8 and (b)–(d) 4 min.

§ The absence of signals corresponding to bound ethoxide suggests the possibility of the substitution of the bound ethoxide by hydroxide (and/or water) groups. Even though no water molecules were observed in the crystal structure, we think that the only possible proton source was from water molecules in the air that were probably physisorbed on the surface of the complex. The presence of such water molecules was inferred from the band at 3.73 (br) ppm in d_6-DMSO. The hydroxyl proton of the unligated $HOCH_2CH_3$ could not explain the observed intensity of this peak, and integration of the peak area suggests the presence of additional protons, most probably from H_2O.

Table 3 A-tensor (G, 10^{-4} cm^{-1}) and g-tensor components of complex **1** in chloroform and DMSO[a]

Solvent	$A_{\parallel}$	$A_{\perp}$	A_{iso}	$g_{\parallel}$	$g_{\perp}$
Chloroform (1.2 mM)[b]	163.0, 148.8	56.5, 52.3	92.0, 84.5	1.955	1.983
DMSO (2.5 mM)[c]	~177.9, ~161.5	—	—	~ 1.945	—
DMSO (0.25 mM)[d]	192.3, 173.9	70.8, 65.4	111.3, 101.6	1.937	1.977

[a] The second-order effect is considered and the values are calculated using the formula developed by Chasteen.[20] [b] See Fig. 6b. [c] Estimated values for the species giving rise to the signals labeled "×" in Fig. 6c. [d] See Fig. 6d.

$\mu_{eff} = 1.79\ \mu_B$ for the complex. The frozen solutions show low-temperature EPR patterns typical of V(IV)=O complexes, where the X-band EPR spectra can be described by axially-symmetric g- and vanadium nuclear hyperfine A-tensors.[20] In most V(IV)=O complexes, the $g_{\parallel}$ and $A_{\parallel}$ axes are almost coincident (within a 10° deviation), which is not resolved in X-band EPR. Each $g_{\parallel}$ and $g_{\perp}$ line splits into eight lines, which are assigned according to the m_I values, shown in Fig. 6b and 6d, from the vanadium(^{51}V, $I = 7/2$) nuclear hyperfine coupling. The second-order effects arising from the large vanadium hyperfine coupling need to be considered to deduce the A- and g-tensor components.[20,21] Table 3 lists the values in each solution state obtained using a previously developed formula.

The EPR spectrum obtained from complex **1** in frozen chloroform is characterized by axial g- and A-tensors, as shown in Table 3 and Fig. 6b. The same solution at room temperature exhibits a slow-motional averaged EPR spectrum owing to the high molecular weight of complex **1**. This gives $A_{iso} \approx 90$ G, which is close to the isotropic hyperfine coupling constant from the frozen solution, indicating that the electron spin is localized on the V(IV)=O site at both temperatures. A low concentration of complex **1** in frozen DMSO shows a stronger hyperfine interaction and a larger g-anisotropy than in chloroform, revealing that the V(IV)-coordination environments are different in the two solvents (Fig. 6d, Table 3). However, at higher concentrations (Fig. 6c), the well-resolved $A_{\parallel}$ lines show additional features (marked by "×" in Fig. 6c) in addition to the signals observed in DMSO at low concentrations, and those from chloroform, demonstrating that three V(IV)=O complexes are in equilibrium in DMSO.

The vanadium hyperfine coupling constant is sensitive to the type of equatorial ligand. The observed $A_{\parallel}$ values can be used to predict the equatorial ligand groups using the additive relationship of $A_{\parallel,calc} = (\Sigma n_i A_{\parallel,i})/4$, developed by Chasteen, where $A_{\parallel,i}$ is the experimentally determined value for ligand i from the model V(IV)=O complexes with all four equatorial ligands having the same i, and n_i is the number of the ligand types in the complex of interest.[20,22,23] For N_2O_2 equatorial donor ligands, a value of $A_{\parallel,calc} = 152.1 \times 10^{-4}$ cm^{-1} was obtained by using $A_{\parallel,i} = 162.8 \times 10^{-4}$ cm^{-1} for the "=N–" ligand, and $A_{\parallel,i} = 141.3 \times 10^{-4}$ cm^{-1} for the "R–O$^-$" ligand.[20] Considering that the above $A_{\parallel,i}$ values were derived from aqueous complexes, and taking into account the sensitivity of the $A_{\parallel,i}$ values to the ligand geometry, this value is reasonably close to the value of $A_{\parallel}$ of complex **1** in chloroform (Table 3), indicating that the data in Fig. 6b arises from the original complex **1** that exists in chloroform. In DMSO, the low concentration solution yields a much higher value of $A_{\parallel} = 173.9 \times 10^{-4}$ cm^{-1} (Table 3). This is close to the calculated value of $A_{\parallel,i}$ of $A_{\parallel} = 178.5 \times 10^{-4}$ cm^{-1} for DMSO,[24] suggesting that the EPR spectrum shown in Fig. 6d is due to a fully solvent-coordinated V(IV)=O species. The value of $A_{\parallel}$ for species "×" lies in-between the $A_{\parallel}$ values of 148.8×10^{-4} cm^{-1} and 173.9×10^{-4} cm^{-1}. This would arise from having either complex **1** with its V(IV)=O axial position occupied by a DMSO molecule, or from another vanadyl species with the equatorial V(IV)=O ligand(s) of complex **1** partially replaced by DMSO.

Complex **1** generates a complicated EPR spectrum in the solid state at room temperature (Fig. 6a). The shortest distance between the two V(IV) centers (V2a–V2) from the crystal data was measured as 5.32 Å (Fig. 3), which can influence the observed EPR spectrum through spin-exchange and dipole–dipole coupling in a biradical. However, spin delocalization through a weak O=V2a(IV)···O=V1(V) coordination cannot be excluded (Fig. 3). A more detailed study of the spin-behavior in the solid state is now in progress.

Summary

We have prepared a trinuclear mixed valence vanadium(V/IV/V) complex, **1**, using an H_3hshz ligand that functioned as a potential trianionic pentadentate chelating ligand (hshz^{3-}). A vanadium(IV) atom is at the center of complex **1**, and is spanned by two terminal vanadium(V) ions with a square pyramidal geometry bridged *via* hydrazido ligands. In the crystalline state, these trinuclear vanadium complexes are linked *via* two different types of linkages to form a linear zigzag chain structure. The oxo group of the central vanadium(IV) ion is weakly coordinated to one of the terminal square pyramidal vanadium(V) ions of the neighboring trinuclear complex. Two oxo-bridges of the same type form the cyclic hexanuclear cluster, which is a dimer of the trinuclear complex. These cyclic hexanuclear clusters are linked *via* bis μ-alkoxo bridges to form a one-dimensional zigzag-type chain. Complex **1** has one unpaired electron with $S = 1/2$, with the spin localized at the V(IV)=O site in both the solid and solvated states. In chloroform, the weak linkages in complex **1** that exist between the trinuclear complexes in the crystalline state are broken, and only the spin localized mixed valence trinuclear complex was identified. However, three different species exist in equilibrium when complex **1** is dissolved in DMSO: one is the form of complex **1** that exists in chloroform, the other is suggested to be a V(IV)=O complex that is fully coordinated by DMSO, and the third form is probably either a form of complex **1** with DMSO occupying the axial V(IV)=O position, or a form where the equatorial V(IV)=O ligand(s) of complex **1** are partially replaced with DMSO.

Acknowledgements

We thank the Korean Institute of Basic Science for the elemental analyses. The authors wish to acknowledge the financial support of the Korea Research Foundation (Grant KRF-2002-070-C00053).

References

1 (*a*) N. D. Chasteen, *Vanadium in Biological Systems*, Kluwer Academic Publishers, Dordrecht, The Netherlands, 1990; (*b*) A. Butler and C. J. Carrano, *Coord. Chem. Rev.*, 1991, **109**, 61–105; (*c*) D. Rehder, *Angew. Chem., Int. Ed. Engl*, 1991, **30**, 148–167.
2 N. D. Chasteen, *Struct. Bonding*, 1983, **53**, 105.
3 K. Kustin, G. C. McLeod, T. R. Gilbert and L. B. R. Briggs, *Struct. Bonding*, 1983, **53**, 139.
4 (*a*) S. K. Dutta, S. Samanta, S. B. Kumar, O. H. Han, P. Burckel, A. A. Pinkerton and M. Chaudhury, *Inorg. Chem.*, 1999, **38**, 1982–1988; (*b*) R. A. Holwerda, B. R. Whittlesey and M. J. Nilges, *Inorg. Chem.*, 1998, **37**, 64–68; (*c*) B. J. Hamstra, A. L. P. Houseman, G. J. Colpas, J. W. Kampf, R. LoBrutto, W. D. Frasch and V. L. Pecoraro, *Inorg. Chem.*, 1997, **36**, 4866–4874; (*d*) A. D. Keramidas, S. N. Miller, O. P. Anderson and D. C. Crans, *J. Am. Chem. Soc.*, 1997, **119**, 8901–8915;

(*e*) S. Mondal, P. Ghosh and A. Chakravorty, *Inorg. Chem.*, 1997, **36**, 59–63; (*f*) G. J. Colpas, B. J. Hamstra, J. W. Kampf and V. L. Pecoraro, *J. Am. Chem. Soc*, 1996, **118**, 3469–3478.
5 C. G. Young and Coord, *Chem. Rev.*, 1989, **96**, 89–251.
6 (*a*) S. K. Dutta, S. Samanta, S. B. Kumar, O. H. Han, P. Burckel, A. A. Pinkerton and M. Chaudhury, *Inorg. Chem.*, 1999, **38**, 1982–1988; (*b*) R. Dinda, P. Sengupta, S. Ghosh and T. C. W. Mak, *Inorg. Chem.*, 2002, **41**, 1684–1688; (*c*) J. C. Pessoa, M. J. Calhorda, I. Cavaco, I. Correia, M. T. Duarte, V. Felix, R. T. Henriques, M. F. M. Piedade and I. Tomaz, *J. Chem. Soc., Dalton Trans.*, 2002, 4407–4415; (*d*) A. Neves, L. M. Rossi, A. J. Bortoluzzi, A. S. Mangrich, W. Haase and O. R. Nascimento, *Inorg. Chem. Commun.*, 2002, **5**, 418–421.
7 (*a*) R. Codd, T. W. Hambley and P. A. Lay, *Inorg. Chem.*, 1995, **34**, 877–882; (*b*) J. W. Johnson, D. C. Johnston, H. E. King, Jr., T. R. Halbert and J. F. Brody, *Inorg. Chem.*, 1988, **27**, 1646–1648.
8 (*a*) K. H. Thompson, J. H. McNeill and C. Orvig, *Chem. Rev.*, 1999, **99**, 2561–2571; (*b*) L. C. Y. Woo, V. G. Yuen, K. H. Thompson, J. H. McNeill and C. Orvig, *J. Inorg. Biochem.*, 1999, **76**, 251–257; (*c*) Y. Shechter, *Lett. Pept. Sci.*, 1998, **5**, 319–322; (*d*) D. Rehder, G. Santoni, G. M. Licini, C. Schulzke and B. Meier, *Coord. Chem. Rev.*, 2003, **237**, 53–63.
9 B. Kwak, H. Rhee and M. S. Lah, *Polyhedron*, 2000, **19**, 3599–3602.
10 D. F. Evans, *J. Chem. Soc.*, 1958, **80**, 2003–2005.
11 *SMART and SAINT, Area Detector Software Package and SAX Area Detector Integration Program*, Bruker Analytical X-ray, Madison, WI, USA, 1997.
12 *SADABS, Area Detector Absorption Correction Program*, Bruker Analytical X-ray, Madison, WI, USA, 1997.
13 G. M. Sheldrick, *SHELXTL-PLUS, Crystal Structure Analysis Package*, Bruker Analytical X-Ray, Madison, WI, USA, 1997.
14 (*a*) S. P. Rath, K. K. Pajak and A. Chakravorty, *Inorg. Chem.*, 1999, **38**, 4376–4377; (*b*) M. Mahroof-Tahir, A. D. Keramidas, R. B. Goldfarb, O. P. Anderson, M. M. Miller and D. C. Crans, *Inorg. Chem.*, 1997, **36**, 1567–1668.
15 (*a*) S. K. Dutta, S. B. Kumar, S. Bhattacharya, E. R. T. Tiekink and M. Chaudhury, *Inorg. Chem.*, 1997, **36**, 4954–960; (*b*) M. Moon, M. Pyo, Y. C. Myoung, C. I. Ahn and M. S. Lah, *Inorg. Chem.*, 2001, **40**, 554–557.
16 (*a*) H. Schmodt, M. Bashirpoor and D. Rehder, *J. Chem. Soc., Dalton Trans.*, 1996, **19**, 3865–3870; (*b*) D. C. Crans, H. Chen, O. P. Anderson and M. M. Miller, *J. Am. Chem. Soc.*, 1993, **115**, 6769–6776; (*c*) W. Priebsch and D. Rehder, *Inorg. Chem.*, 1990, **29**, 3013–3019; (*d*) W. Plass, *Inorg. Chim. Acta*, 1996, **244**, 221–229.
17 (*a*) G. Asgedom, A. Sreedhara and C. P. Rao, *Polyhedron*, 1995, **14**, 1873–1879.
18 G. Asgedom, A. Sreedhara, J. Kivikoski, E. Kolehmain-nen and C. P. Rao, *Inorg. Chem.*, 1996, **35**, 5674–5683.
19 (*a*) J. Dai, H. Wang and M. Mikuriya, *Polyhedron*, 1996, **15**, 1801–1806; (*b*) H. Hagen, A. Barbon, E. E. van Faassen, B. T. G. Lutz, J. Boersma, A. L. Spek and G. van Koten, *Inorg. Chem.*, 1999, **38**, 4079–4086.
20 N. D. Chasteen, *Biological Magnetic Resonance*, ed. J. Reuben, Plenum Press, New York, USA, 1981, pp. 53–119.
21 A. Abragam and B. Bleaney, *Electron Paramagnetic Resonance of Transition Ions*, Clarendon Press, Oxford, UK, 2nd edn., 1970.
22 K. Wurthrich, *Helv. Chim. Acta*, 1965, **48**, 1012.
23 T. S. Smith, C. A. Root, J. W. Kampf, P. G. Rasmussen and V. L. Pecoraro, *J. Am. Chem. Soc.*, 2000, **122**, 767–775.
24 R. Ando, M. Nagai, T. Yagyu and M. Maeda, *Inorg. Chim. Acta*, 2003, **351**, 107–113.